

1 **Published in TREES – Structure and Function Oct 2015**

2 DOI 10.1007/s00468-015-1301-5

3 **Xylem traits and water-use-efficiency of co-occurring woody species from**
4 **the Ti Tree Basin arid zone**

5

6 Nadia S. Santini¹, James Cleverly¹, Rolf Faux¹, Catherine Lestrange¹, Rizwana
7 Rumman¹, Derek Eamus¹

8

9 ¹Terrestrial Ecohydrology Research Group, University of Technology Sydney, PO
10 Box 123, NSW 2007, Australia.

11

12 Corresponding author

13 nadiasilvanasantini@gmail.com

14

15 **Abstract**

16 The hydraulic niche separation theory proposes that species co-exist by having a
17 range of traits to allow differential access to resources within heterogeneous
18 environments. Here, we examined variation in branch xylem anatomy and foliar
19 carbon stable isotopes ($\delta^{13}\text{C}$) as a measure of water-use-efficiency (WUE) in
20 seven co-occurring species, *Acacia aneura*, *Acacia bivenosa*, *Corymbia opaca*,
21 *Eucalyptus camaldulensis*, *Erythrina vespertillo*, *Hakea* sp., and *Psyrax latifolia*, in
22 an arid zone open *Corymbia* savanna on the Ti Tree Basin, Northern Territory,
23 Australia. We test the following hypotheses: (1) Species with large conductive
24 areas exhibit a low density of intact branches, while species with small
25 conductive areas have a significantly higher density of intact branches. (2)
26 Species with smaller conductive areas exhibit more enriched values of $\delta^{13}\text{C}$ and
27 therefore have larger WUE than those with larger conductive areas and (3) there
28 is an inverse correlation between theoretical sapwood hydraulic conductivity
29 and vessel implosion resistance. The results of this study demonstrated
30 significant variation in density of intact branches, ranging from 0.38 g cm^{-3} to
31 0.80 g cm^{-3} and this variation was largely explained by variation in sapwood
32 conductive area. Species with low conductive areas (*P. latifolia*, *Hakea* sp. and
33 *Acacia* species) exhibited large values of WUE ($r^2=0.62$, $p<0.05$). These species

34 are likely to be less vulnerable to cavitation by having small conductive areas
35 and thicker fibre walls. We demonstrated a significant ($r^2=0.83$, $p=0.004$)
36 negative correlation between theoretical sapwood hydraulic conductivity and
37 vessel implosion resistance. These results are discussed in relation to hydraulic
38 niche separation.

39

40 **Keywords**

41 Wood-anatomy, hydraulic niche separation, arid zone, water-use-efficiency, ,
42 carbon-isotopes.

43

44 **Key Message**

45 Species with low-density-of-intact-branches are likely to have higher growth
46 rates than species with high-density-of-intact-branches, but at the cost of a lower
47 water-use-efficiency and larger sensitivity to xylem embolism.

48

49 **1. Introduction**

50

51 The theory of hydraulic niche separation proposes that different plant species
52 can co-occur because they can each access a given resource, such as water or
53 nutrients, by utilising different strategies to access these resources under a
54 heterogeneous environment (Silvertown et al. 1999; Silvertown 2004). For
55 example, Terradas et al. (2009) demonstrated in a Mediterranean climate that
56 plant species with deep roots can continuously access groundwater resources,
57 while plant species with shallow roots can only access episodic rainwater. In
58 arid environments such as the Ti Tree basin, Northern Territory, water is a
59 limiting resource and variability in xylem hydraulic traits may be crucial for
60 species co-occurrence within the region.

61

62 Xylem characteristics such as density of intact branch, vessel size and fibre
63 dimensions can influence water transport efficiency and resistance to drought-
64 induced cavitation (Hacke et al. 2001; Chave et al. 2009; Lachenbruch and
65 McCulloh 2014). Thus, variation of xylem traits forms part of the suite of
66 strategies available to support hydraulic niche separation (e.g. Sterck et al.
67 2011). Water transport in plants is significantly influenced by xylem vessel size
68 (Enquist et al. 1999; Tyree and Ewers 1991; Chave et al. 2009). Plants that can
69 continuously access water, such as those depending on groundwater, are
70 expected to exhibit large diameter xylem vessels, low density of intact branches
71 and low resistance to water flow with concomitant large rates of transpiration,
72 carbon gain and growth (King et al. 2006). However, large diameter xylem
73 vessels also increase the risk of cavitation (Hacke et al. 2001). Plants occurring in
74 xeric environments often have narrow xylem vessels and a high density of intact
75 branches, traits which increase the resistance to water flow and decrease plant
76 transpiration rates and growth. However, narrow xylem vessels also decrease
77 their vulnerability to drought-induced cavitation (Groom 2004; Froend and
78 Drake 2006). Furthermore, thicker vessel and fibre walls can also improve xylem
79 resistance to cavitation because of their larger resistance to the mechanical
80 stresses associated with the development of large negative xylem water pressure
81 during drought (Hacke et al. 2001; Pratt et al. 2007; Chave et al. 2009).

82

83 Water-use-efficiency (WUE) can be defined as the ratio of net photosynthesis to
84 transpiration (Farquhar and Richards 1984; Eamus 1991). WUE is correlated
85 with enriched $\delta^{13}\text{C}$ (i.e. larger values of $\delta^{13}\text{C}$, a measure of the ratio of the stable
86 isotopes of carbon ^{13}C and ^{12}C) in photosynthates of leaves and phloem of twigs
87 and stems (Farquhar 1983; Marshall et al. 2007; Gessler et al. 2009). Plant
88 species with high density of intact branches and small xylem vessels are likely to
89 have a larger WUE (due to their low transpiration rates) and larger resistance to
90 drought induced cavitation. Alternatively, species with low density of intact
91 branches are likely to have a lower WUE and to exhibit larger growth rates but at
92 the cost of larger vulnerability to xylem embolism (Enquist et al. 1999; Jacobsen
93 et al. 2005).

94

95 In this study, we examined variation in branch xylem anatomical traits, i.e.,
96 density of intact branches, wood density, conductive area and fibre and vessel
97 wall thickness of seven co-occurring species from the Ti Tree Basin. This basin,
98 with annual average rainfall of approximately 347 mm y^{-1} is classified as an arid
99 basin (Eamus 2003; O' Grady et al. 2009). From our measurements, we
100 determined potential hydraulic conductivity (Zanne et al. 2010), theoretical
101 resistance to vessel implosion (Hacke et al. 2001) and a drought vulnerability
102 index (Carlquist 1977). We also examined foliar carbon stable isotopes ($\delta^{13}\text{C}$) as
103 a measure of WUE to examine the relationship between variation of xylem traits
104 and WUE. We tested the following hypotheses: (1) Species with large conductive
105 areas exhibit a low density of intact branches, while species with small
106 conductive areas have a significantly higher density of intact branches. (2)
107 Species with smaller conductive areas exhibit more enriched values of $\delta^{13}\text{C}$ and
108 therefore have larger WUE than those with larger conductive areas and (3) there
109 is an inverse correlation between theoretical sapwood hydraulic conductivity
110 and vessel implosion resistance.

111

112

113 **2. Materials and Methods**

114

115 **2.1 Site description and sample collection**

116

117 The study site was located in the Ti Tree Basin (22° 7'48. 56"S, 133°24'57. 67"E),
118 approximately 180 km north of Alice Springs, Northern Territory, Australia. The
119 site is arid with a mean annual rainfall of 347 mm y⁻¹ (Bureau of Meteorology,
120 BoM station 15507), most of which falls in monsoonal summer storms. Mean
121 minimum and maximum annual temperatures are 15°C and 31°C respectively.
122 The site reaches maximum air temperatures of > 40 °C in the summer months
123 (December – February). The Ti Tree Basin extends over 5500 km² and contains
124 the ephemeral Hanson and Woodforde rivers, which only flow after intense
125 storms (Harrington et al. 2002).

126

127 During July – September 2014, we collected upper canopy terminal branches of
128 seven co-occurring woody species from the Ti Tree Basin: *Acacia aneura*, *Acacia*
129 *bivenosa*, *Corymbia opaca*, *Eucalyptus camaldulensis*, *Erythrina vespertillo*, *Hakea*
130 *sp.*, and *Psyrdrax latifolia*. Branches of different species varied in diameter (2 – 7
131 mm), but we standardized our collection by sampling the terminal 25 cm of each
132 branch.

133

134 **2.2 Measurement of xylem traits**

135

136 Branches were collected and stored in sealed vials containing 50% ethanol.
137 Cross sections of each branch were fixed in formalin-acetic acid-alcohol (FAA)
138 for 7 days and then placed in 70 % ethanol for two days; we repeated this
139 washing process twice. Micro-sections of all species with the exception of *E.*
140 *vespertillo*, were prepared with a sledge Leica SM2010R microtome. Micro-
141 sections of *E. vespertillo* were pre-treated with ethanol (8 hours), xylene (4
142 hours) and finally embedded in paraffin with a Shandon Histocentre 3 histology-
143 embedding centre (Thermo Fisher Scientific, Australia) before cutting with a
144 Microm HM325 rotatory microtome (Thermo Fisher Scientific, Australia). Micro-
145 sections of all species were double stained with safranin - alcian blue. We
146 photographed the micro-sections with a Leica DM750 microscope and used the
147 software Image J 1.48v (National Institutes of Health, USA) to measure xylem

148 traits. We determined the minor (*a*) and major (*b*) axis diameters of xylem
149 vessels to calculate vessel area (VA) following Eq (1). We also determined vessel
150 density (VD) (Eq 2) to calculate conductive area (CA) of each species as in Eq (3)
151 (Lewis 1992):

$$153 \quad VA = \pi ab0.25 \quad \text{Eq (1)}$$

154

$$155 \quad VD = \frac{\# \text{vessels}}{\text{mm}^2} \quad \text{Eq (2)}$$

156

$$157 \quad CA = VA VD \quad \text{Eq (3)}$$

158

159 We measured fibre wall thickness by measuring the width of 30 – 50 adjoining
160 fibre walls and dividing the total distance by two (Santini et al. 2012). We also
161 assessed vessel wall thickness by measuring double-vessel walls of 20 – 30
162 vessels per species and dividing the total distance by two.

163

164 ***2.3 Potential hydraulic conductivity, resistance to vessel implosion and a*** 165 ***vulnerability index***

166 We calculated the potential hydraulic conductivity (K_s) as in Eq (4):

167

$$168 \quad K_s \propto F^{1.5} S^{0.5} \quad \text{Eq (4)}$$

169 Where F is the vessel fraction and S is the ratio of vessel size to vessel number,
170 calculated as in Eq (5) and (6) (Zanne et al. 2010):

171

$$172 \quad F = VA VD \quad \text{Eq (5)}$$

$$173 \quad S = \frac{VA}{VD} \quad \text{Eq (6)}$$

174

175 Vessel implosion resistance was calculated as:

176

$$177 \quad (t/b)^2 \quad \text{Eq (7)}$$

178

179 Where t is the double-wall thickness and b is the hydraulic mean vessel
180 diameter, both expressed in μm (Hacke et al. 2001).

181

182 Finally, we determined a drought vulnerability index (VI) by dividing vessel
183 diameter (D_h) by vessel density (Carlquist 1977) Eq (8) and (9):

184

$$185 \quad VI = \frac{D_h}{VD} \text{ where } D_h \text{ is,} \quad \text{Eq (8)}$$

186

$$187 \quad D_h = \sqrt{\frac{2a^2b^2}{a^2 + b^2}} \quad \text{Eq (9)}$$

188

189 The vulnerability index is a measure of the redundancy of the number of vessels
190 present per unit sapwood area. A low value is taken to indicate a large resistance
191 to drought (Carlquist 1977).

192

193

194 ***2.4 Density of intact branches and wood density***

195

196 Material to measure density of intact branches and wood density was stored in
197 paper bags and was maintained cool in an insulated container until laboratory
198 analysis. Density of intact branches was measured from ~ 5 cm length branch
199 segments. Branches were placed in water for two days to obtain full branch
200 hydration. We measured the mass of the displaced hydrated branch. The same
201 branches were oven dried for 5 days at 60°C to attain constant weight. Density of
202 intact branches was calculated by dividing dry mass by hydrated branch volume.
203 Wood density was measured following the same methods as for measuring
204 density of intact branches but after carefully debarking our intact branches with
205 a razor blade.

206

207 ***2.5 Analysis of stable carbon isotopes $\delta^{13}\text{C}$***

208

209 Samples stored in paper bags were completely dried in an oven at 60°C for 5
 210 days. Dry leaf samples were ground with a Retsch MM300 grinding mill (Verder
 211 Group, Netherlands). The ground material was placed in 3.5 mm x 5 mm tin
 212 capsules for analysis of $\delta^{13}\text{C}$. Analyses were performed with a Picarro G2121-i
 213 Analyser (Picarro, Santa Clara, CA, USA) for isotopic CO_2 . Values of $\delta^{13}\text{C}$ were
 214 quantified as in Eq (10), where R corresponds to the isotopic value $^{13}\text{CO}_2/^{12}\text{CO}_2$
 215 of the sample (R_a) or the standard (R_b). We used atropine and acetanilide as
 216 laboratory standard references. Results were normalized with the international
 217 standards sucrose (IAEA-CH-6, $\delta^{13}\text{C}_{\text{VPDB}} = -10.45$), cellulose (IAEA-CH-3, $\delta^{13}\text{C}_{\text{VPDB}}$
 218 = -24.72) and graphite (USGS24, $\delta^{13}\text{C}_{\text{VPDB}} = -16.05$).

$$220 \quad \delta^{13}\text{C} = \left(\frac{R_a}{R_b} - 1\right) \times 1000 \quad \text{Eq (10)}$$

221

222

223 **2.6 Data analyses**

224

225 We used linear regression analyses to test the relationships between density of
 226 intact branches and conductive area, vessel area and fibre wall thickness, vessel
 227 density and fibre wall thickness, potential hydraulic conductivity and log (vessel
 228 implosion resistance) and density of intact branches and wood density. One-way
 229 ANOVA tests were used to compare values of density of intact branches,
 230 conductive area, fibre wall thickness, vessel wall thickness, $\delta^{13}\text{C}$, theoretical
 231 hydraulic conductivity, vessel implosion resistance and vulnerability index
 232 between species. We used a paired t-test to compare mean and standard errors
 233 of density of intact branches and wood density within species.

234

235 We used $\delta^{13}\text{C}$ of leaves to calculate water-use-efficiency (WUE) following Eq (11)
 236 and Eq (12) (Marshall et al. 2007):

237

$$238 \quad WUE_i = \frac{c_a(b - \Delta)}{1.6(b - a)} \quad \text{Eq (11)}$$

239

240 Where c_a is the atmospheric concentration of CO_2 , which is ~ 390 ppm, a
241 corresponds to discrimination of $^{13}\text{CO}_2$ due to slower motion from the
242 atmosphere through the leaf stomata (~ -4.4 ‰) and b is the discrimination
243 against $^{13}\text{CO}_2$ molecules from the enzyme ribulose biphosphate
244 carboxylase/oxygenase within the leaf (~ -27 ‰). The Δ value was calculated as:
245

$$246 \quad \Delta = (\delta^{13}\text{C}_{\text{atm}} - \delta^{13}\text{C}_{\text{plant}}) / (1 + \frac{\delta^{13}\text{C}_{\text{plant}}}{1000}) \quad \text{Eq (12)}$$

247

248 Where $\delta^{13}\text{C}_{\text{atm}}$ is -8.1 ‰ (Carbon Dioxide Information Analysis Center 2014) and
249 $\delta^{13}\text{C}_{\text{plant}}$ are the values obtained from leaves as indicated in Eq (10).

250

251 We determined the relationship between WUE and conductive area with a
252 Spearman correlation analysis. All analyses were performed using Prism version
253 6.0a (GraphPad Software, La Jolla, CA, USA) and the R software package,
254 functions *glm* and *lm* (R Development Core Team 2008).

255

256 **3. Results**

257

258 **3.1 Xylem traits**

259

260 The density of intact branches was significantly lower in *E. vespertillo* than in five
261 of the six remaining species (Table 1) whilst the density of intact branches of *C.*
262 *opaca* was significantly lower than four of the remaining species (Table 1).

263

264 Fibre wall thickness was significantly larger in *P. latifolia* than the remaining six
265 species (*E. vespertillo*, *C. opaca*, *E. camaldulensis*, *Hakea* sp., *A. aneura* and *A.*
266 *bivenosa*) (Table 1). Vessel wall thickness was highest in *A. bivenosa*, *A. aneura*
267 and *P. latifolia* and lowest in *E. vespertillo* (Table 1). Conductive areas per mm^2 of
268 cross section of branch varied from $0.098 \pm 0.008 \text{ mm}^2 \text{ mm}^{-2}$ in *A. aneura* to
269 $0.258 \pm 0.053 \text{ mm}^2 \text{ mm}^{-2}$ in *E. camaldulensis* (Table 1).

270

271 Density of intact branches was largely explained by xylem conductive area ($r^2 =$
272 0.83 ; $p = 0.004$, Fig. 1). Thus species in which vessel size and vessel density
273 combine as larger conductive areas also exhibited a lower density of intact
274 branches. There was a significant negative relationship between vessel area and
275 fibre wall thickness ($r^2 = 0.80$; $p = 0.006$, Fig. 2). We found a positive relationship
276 between vessel density and fibre wall thickness ($r^2 = 0.61$; $p = 0.037$, Fig. S1).
277 However, when *P. latifolia* was excluded from the analysis, the regression was
278 not significant ($r^2 = 0.05$; $p = 0.6$, Fig. 3).

279

280 Values of potential hydraulic conductivity (K_s) were significantly larger ($p < 0.05$)
281 in *E. vespertillo*, *C. opaca* and *E. camaldulensis* compared to *P. latifolia*, *Hakea* sp.,
282 *A. aneura* and *A. bivenosa* (Table 3).

283

284 The theoretical resistance to vessel implosion $(t/b)^2$ ranged from $0.0096 \pm$
285 0.00006 in *E. vespertillo* to 0.14 ± 0.00092 in *P. latifolia* (Table 3). There was a
286 significant negative log linear relationship between potential hydraulic
287 conductivity and resistance to vessel implosion ($r^2 = 0.83$; $p = 0.004$, Fig. 4) across
288 the seven species.

289

290 The Vulnerability index (VI) was significantly larger in *A. aneura* and *A. bivenosa*
291 compared to most other species (Table 3).

292

293 Our paired t-test analysis to compare density of intact branches and wood
294 density showed that in five of our seven species: *C. opaca*, *E. camaldulensis*, *P.*
295 *latifolia*, *Hakea* sp. and *A. aneura*, wood density was significantly higher ($p < 0.05$)
296 than the density of intact branches. However, in *E. vespertillo* and in *A. bivenosa*
297 differences between density of intact branch and wood density were not
298 significant (Table 1). Density of intact branches and wood density exhibited a
299 large positive correlation coefficient ($r^2 = 0.93$, $p = 0.0003$, Fig. 5).

300

301

302 **3.2 Stable carbon isotopes $\delta^{13}C$**

303

304 Values of $\delta^{13}\text{C}$ from leaves were significantly more depleted in *E. camaldulensis*
305 than five of the remaining six species whilst there were no significant differences
306 amongst the remaining six species (Table 2). There was a significant negative
307 correlation between water-use-efficiency and conductive area ($r^2=0.81$, $p<0.05$,
308 Fig. 6).

309

310 **4. Discussion**

311

312 Density of intact branches was highly variable across the seven co-occurring
313 species from the arid zone Ti Tree Basin. Density of intact branches values
314 ranged from $0.38 \pm 0.007 \text{ g cm}^{-3}$ in *E. vespertillo* to $0.80 \pm 0.03 \text{ g cm}^{-3}$ in *A.*
315 *bivenosa*. These values agree with previous results of O'Grady et al. (2009) who
316 observed a similar range for their 12 species study in arid Australia. This large
317 variation in values reflects the variability in a number of anatomical and
318 functional traits. Anatomical characteristics determining density, including
319 conductive areas and fibre content, influence the hydraulic and mechanical
320 properties of woody plants (Santini et al. 2012; Lachenbruch and McCulloh
321 2014). Our linear regression analysis indicated that variation in density of intact
322 branches was largely explained by differences in conductive areas across
323 species. *Acacia bivenosa* and *A. aneura* had the highest density and also exhibited
324 the smallest conductive areas, while *E. vespertillo*, *E. camaldulensis* and *C. opaca*
325 exhibited lower density and larger conductive areas. The negative relationship
326 between density of intact branch and conductive area is in agreement with our
327 first hypothesis and with previous studies (Chave et al. 2009; Lachenbruch and
328 McCulloh 2014 and references therein). This relationship may reflect that
329 species with larger conductive areas (*E. camaldulensis*, *C. opaca* and *E.*
330 *vespertillo*) may also exhibit larger growth rates compared to those species with
331 smaller conductive areas (*A. aneura*, *A. bivenosa*, *P. latifolia* and *Hakea* sp.).
332 Larger growth rates in species with larger conductive areas are likely to be due
333 to larger lumen areas enabling larger transpiration rates and concomitant larger
334 rates of carbon gain (Enquist et al. 1999). O'Grady et al. (2009) found that *E.*
335 *camaldulensis*, which has large conductive areas, exhibited significantly larger
336 rates of water use and larger specific leaf areas (the ratio of leaf area to leaf dry

337 weight) than *A. aneura*, that has small conductive areas. In addition, we found
338 that *E. vespertillo*, *C. opaca* and *E. camaldulensis* exhibited larger theoretical
339 hydraulic conductivities compared to *Acacia* species, *Hakea* sp. and *Psyrax*
340 *latifolia*, further suggesting that the three former species will exhibit larger
341 transpiration rates and hence larger growth rates than the three latter species.
342 Given that growth and photosynthetic rate correlate with specific leaf area and in
343 many cases determine plant productivity, these findings and our results of
344 potential hydraulic conductivity (Table 3; Martínez-Cabrera and Estrada-Ruiz
345 2014) support our second hypothesis, that species with larger conductive areas
346 and lower density of intact branch utilize more water and gain more carbon than
347 species with lower density of intact branch (Kriedeman 1986; Enquist et al.
348 2007; Cornelissen et al. 2003).

349

350 We determined a significant negative relationship between intrinsic water-use-
351 efficiency and conductive area. High WUE is associated with slow growth
352 species that exhibit low transpiration rates (Ball 1988; Hasselquist et al. 2010;
353 Craven et al. 2013; Table S1). Our results indicated that *Acacia* species, *Hakea* sp.
354 and *P. latifolia*, characterized by small conductive areas, small potential
355 hydraulic conductivities and larger resistance to vessel implosion exhibited a
356 large WUE. These species are also characterized by their low stature in the field
357 and extreme tolerance of very low soil and foliar water potentials (< -6 MPa).
358 Furthermore, *Acacia* species have shallow roots, which can laterally extend 13 m
359 and can only access shallow soil water in our study site (Dunkerley 2002; Rolf
360 Faux field observation). In contrast, *E. camaldulensis* is known to access the
361 shallow (< 3 m) groundwater at our riparian site in the Ti-Tree (O'Grady et al.
362 2009; Rolf Faux field observation). High WUE and high density of intact
363 branches for *Acacia* spp., *Hakea* sp. and *P. latifolia* are likely to contribute
364 significantly to their tolerance of aridity in the Ti Tree Basin, where a thick fibre
365 matrix, small conductive areas and large vessel implosion resistance confer a
366 larger resistance to xylem embolism. Our results support our third hypothesis
367 that there is an inverse correlation between theoretical sapwood hydraulic
368 conductivity and vessel implosion resistance. The pre-dawn and mid-day foliar
369 water potential of *Acacia* spp. is much lower than that of several co-occurring

370 tree species (especially *E. camaldulensis*; O'Grady et al. 2009), indicative of an
371 effective drought tolerant strategy for such species. Additionally, a low specific
372 leaf area in *Acacia* spp. may help them to avoid excessive water loss (O'Grady et
373 al. 2006; O'Grady et al. 2009). In contrast, *E. camaldulensis*, *C. opaca* and *E.*
374 *vespertillo* exhibited low WUE (Table 2) and these species access shallow
375 groundwater (O'Grady et al. 2009). In these phreatophytic species, where water
376 is not a limiting resource, larger conductive areas and transpiration rates do not
377 compromise their hydraulic safety (O'Grady et al. 2009) and support the large
378 growth form of these species.

379

380 Wood density was correlated with density of intact branches ($r^2=0.93$,
381 $p=0.0003$). However, wood density was significantly higher than the density of
382 intact branches in most species. These results agree with Santini et al. (2012)
383 that found that bark in small branches is less dense than sapwood and do not
384 contribute to mechanical support. Our results indicate that in small branches (~
385 2 – 7 mm diameter) density of intact branch can be used as a proxy for wood
386 density. In species from the Ti Tree Basin bark may be important in protection
387 from high temperatures; inner bark has also been demonstrated to play a role in
388 reducing water loss and in isolating tree stems from heat (Pausas 2014).

389

390 Wood density has been correlated with resistance to pathogen invasion and
391 higher survival, but this may be at the cost of reduced growth rates and low
392 water storage capacitance of wood, important for maintaining cell turgidity
393 (Bucci et al. 2004; Scholz et al. 2007; Meinzer et al. 2008). Therefore branches of
394 *A. bivenosa* and *A. aneura* which had the highest values of density of intact
395 branches may survive longer than branches of *E. vespertillo*, but this may be at
396 the cost of low growth rates and low water storage capacitance.

397

398 There was a significant negative relationship between vessel area and fibre wall
399 thickness (Fig. 2) that may indicate that vessel area is not crucial in determining
400 the mechanical support within the plant water transport system.

401

402 Although we found a positive trend between density of intact branches and fibre

403 wall thickness, the regression was not significant. Previous studies (Jacobsen et
404 al., Santini et al. 2012, Chave et al. 2009, Zieminska et al. 2013) have found that
405 fibres largely determine wood density. Our study only accounted for fibre wall
406 thickness, but partitioning and arrangement of fibres is also likely to be an
407 important characteristic that determines wood density (Zieminska et al. 2013).
408 *Acacia aneura* and *A. bivenosa*, which exhibited the highest density of intact
409 branches did not have the thickest fibres but these species did form large fibre
410 clusters. *Acacia* species also have little parenchyma tissue and thick vessel walls
411 (Table 1); these characteristics are likely to account for density of intact
412 branches (IAWA 2014).

413

414 Carlquist (1977) proposed a drought vulnerability index (VI), calculated as mean
415 vessel diameter divided vessel density. The correlation of this VI and resistance
416 to drought can be low, such as the correlation of ecosystem average VI with
417 rainfall across a West Australia rainfall gradient is poor ($r^2 = 0.32$; Carlquist
418 1977). Poor correlations might be explained by the importance of traits other
419 than vessel diameter and vessel density, including larger vessel wall thickness
420 and larger groupings of vessels into clusters, however in our species the
421 correlation between vessel wall thickness and VI was not significant. In the
422 present study, the largest VI was observed in the two *Acacia* species. This is
423 contrary to what we know about *Acacia* species, which is that they tolerate
424 aridity extremely well, and transpire even when foliar water potentials are less
425 than -6 MPa (O'Grady et al. 2009) and their density of intact branch is
426 significantly higher than that of *E. camaldulensis* (Table 1). Therefore, we
427 conclude that at least in the current study, the calculation of VI as *per* Carlquist
428 (1977) does not generate a true representation of vulnerability to drought.

429

430 **5. Conclusions**

431

432 This research advances our understanding on how different woody traits play a
433 specific role in driving hydraulic niche separation of co-occurring species. Our
434 results support the hypothesis that density of intact branch negatively correlates
435 with sapwood conductive area. In addition, our results support the idea that

436 xylem hydraulic traits contribute to the set of strategies that allow species co-
437 occurrence under heterogeneous environments. *Erythrina vespertillo*, *C. opaca*
438 and *E. camaldulensis* with their lower density of intact branches, larger
439 conductive areas, thinner fibre walls, small resistance to vessel implosion and
440 deeper root systems (O'Grady *et al.* 2009, Rolf Faux field observation) are reliant
441 on constantly accessing groundwater resources at the cost of low resistance to
442 cavitation and low WUE but larger growth rates. In contrast, *P. latifolia*, *Hakea*
443 sp. and *Acacia* species that access episodic rain water with their shallow root
444 systems (Rolf Faux field observation), are likely to be less vulnerable to
445 cavitation by having a high density of intact branch, smaller conductive area,
446 thicker fibre walls and high vessel implosion resistance. Associated with these
447 traits is a larger WUE, but possibly, a reduced rate of growth.

448

449 **Aknowledgements**

450

451 We would like to thank the Endeavour Fellowships Scope Global, Australia for
452 financial support (Grant number ERF_PDR_4065_2014). We also thank Dr.
453 Sebastian Pfautsch from the University of Western Sydney. Jacqueline Loyola-
454 Echeverría, Dr. Rachael Nolan and Tonantzin Tarin-Terrazas from the University
455 of Technology Sydney, Dr. Nele Schmitz from the École Normale Supérieure de
456 Lyon and Dr. Kasia Ziemińska from Macquaire University for laboratory
457 assistance and advice during the planning and development of this study. This
458 work was also supported by an ARC grant (DP140101150) awarded to Derek
459 Eamus.

460

461 **Author contribution**

462

463 NSS performed the laboratory work, analyzed the data, wrote the first
464 manuscript draft and designed the study. DE designed the study, contributed
465 reagents and materials and critically revised the manuscript. RR contributed
466 with $\delta^{13}\text{C}$ data from leaves and provided laboratory assistance. JC and RF
467 collected the plant material. CL contributed with laboratory work.

468

469

470 **Conflict of interest**

471 The authors declare they have no conflict of interest.

472

473 **References**

474

475 Australian Bureau of Meteorology (2014) Australian Bureau of Meteorology

476 home page. Commonwealth of Australia: Canberra.

477 <http://www.bom.gov.au>. Accessed 1 November 2014.

478

479 Ball MC (1988) Salinity tolerance in the mangroves *Aegiceras corniculatum* and

480 *Avicennia marina* I. Water use in relation to growth, carbon

481 partitioning, and salt balance. *Aust J Plant Physiol.* 15:447 –

482 464. Doi:10.1071/PP9880447

483

484 Bucci SJ, Goldstein G, Meinzer FC, Scholz FG, Franco AC, Bustamante M (2004)

485 Functional convergence in hydraulic architecture and water

486 relations of tropical savanna trees: from leaf to whole plant.

487 *Tree Physiol.* 24: 891 – 899. doi: 10.1093/treephys/24.8.891

488

489 Carbon Dioxide Information Analysis Center (2014) <http://cdiac.ornl.gov/>.

490 Accessed 1 September 2014.

491

492 Carlquist S (1977) Ecological factors in wood evolution: A floristic approach. *Am*

493 *J Bot.* 64: 887 – 896.

494

495 Chave J, Coomes D, Jansen S, Lewis SL, Swenson NG, Zanne AE (2009) Towards a

496 worldwide wood economics spectrum. *Ecol Lett.* 12: 351 –

497 366. doi:10.1111/j.1461-0248.2009.01285.x

498

499 Craven D, Hall JS, Ashton MS, Berlyn GP (2013) Water use efficiency and whole

500 plant performance of nine tropical tree species at two sites

501 with contrasting water availability in Panama. *Trees*. 27:639
502 – 653. doi: 10.1007/s00468-012-0818-0
503
504 Cornelissen JHC, Lavorel S, Garnier E, Diaz S, Buchmann N, Gurvich DE, Reich PB,
505 Steege H, Morgan HD, van der Heijden MGA, Pausas JG,
506 Poorter H (2003) A handbook of protocols for standardized
507 and easy measurement of plant functional traits worldwide.
508 *Aust J Bot*. 51: 335 – 380. doi: 10.1071/BT02124
509
510 Dunkerley D (2002) Systematic variation of soil infiltration rates within and
511 between the components of the vegetation mosaic in an
512 Australian desert landscape. *Hydrol Process*. 16: 119 – 131.
513 doi: 10.1001/hyp.357
514
515 Eamus D (1991) The interaction of rising CO₂ and temperatures with water use
516 efficiency. *Plant Cell Environ*. 14: 843 – 852. doi:
517 10.1111/j.1365-3040.1991.tb01447.x
518
519 Eamus D (2003) How does ecosystem water balance affect net primary
520 productivity of woody ecosystems? *Funct Plant Biol*. 30:187–
521 205. doi: 10.1071/FP02084
522
523 Enquist B, West G, Charnov E, Brown J (1999) Allometric scaling of production
524 and life-history variation in vascular plants. *Nature* 401:
525 909–911. doi:10.1038/44819
526
527 Enquist BJ, Kerkhoff AJ, Stark SC, Swenson NG, McCarthy MC, Price CA (2007) A
528 general integrative model for scaling plant growth, carbon
529 flux, and functional trait spectra. *Nature*. 449:218 – 222. doi:
530 10.1038/nature06061
531

532 Farquhar GD, Richards RA (1983) Isotopic composition of plant carbon
533 correlates with water use efficiency of wheat genotypes. Aust
534 J Plant Physiol. 11: 539 – 552. doi:10.1071/PP9840539
535

536 Froend RH, Drake PL (2006) Defining phreatophyte response to reduced water
537 availability: preliminary investigations on the use of xylem
538 cavitation vulnerability in *Banksia* woodland species. Aus J
539 Bot. 54: 173-179. <http://dx.doi.org/10.1071/BT05081>.
540

541 Gessler A, Brandes E, Buchmann N, Helle G, Rennenberg H, Barnard RL (2009)
542 Tracing carbon and oxygen isotope signals from newly
543 assimilated sugars in the leaves to the tree-ring archive. Plant
544 Cell Environ. 32:780 – 795. doi: 10.1111/j.1365-
545 3040.2009.01957.x
546

547 Groom PK (2004) Rooting depth and plant water relations explain species
548 distribution patterns within a sandplain landscape. Func
549 Plant Biol. 31: 423-428. doi:10.1071/FP03200.
550

551 Hacke UG, Sperry JS, Pockman WT, Davis SD, McCulloh KA (2001) Trends in
552 wood density and structure are linked to prevention of xylem
553 implosion by negative pressure. Oecologia. 126: 457 – 461.
554 doi: 10.1007/s004420100628
555

556 Harrington GA, Cook PG, Herczeg AL (2002) Spatial and temporal variability of
557 groundwater recharge in Central Australia: A tracer
558 approach. Groundwater. 40: 518-528. doi:10.1111/j.1745-
559 6584.2002.tb02536.x
560

561 Hasselquist N, Allen M, Santiago L (2010) Water relations of evergreen and
562 drought-deciduous trees along a seasonally dry tropical
563 forest chronosequence. Oecologia 164:881–890. doi:
564 10.1007/s00468-012-0818-0

565

566 International Association of Wood Anatomists (IAWA) (2014).

567 <http://bio.kuleuven.be/sys/iawa/>. Accessed 5 May 2015.

568

569 Jacobsen AL, Ewers FW, Pratt B, Paddock WA, Davis SD (2005) Do xylem fibres

570 affect vessel cavitation resistance? *Plant Physiol.* 139: 546 –

571 556. doi: <http://dx.doi.org/10.1104/pp.104>.

572

573 King DA, Davies SJ, Tan S, Noor NSM (2006) The role of wood density and stem

574 support costs in the growth and mortality of tropical trees. *J*

575 *Ecol.* 94: 670 – 680. doi:10.1111/j.1365-2745.2006.01112.x

576

577 Kriedemann, PE (1986) Stomatal and photosynthetic limitations to leaf growth.

578 *Aust J Plant Physiol.* 13, 15-32.

579

580 Lachenbruch B, McCulloh KA (2014) Traits, properties, and performance: how

581 woody plants combine hydraulic and mechanical functions in

582 a cell, tissue, or whole plant. *New Phytol.* 204: 747 – 764.

583 doi:10.1111/nph.13035.

584

585 Lewis AM (1992) Measuring the hydraulic diameter of a pore or conduit. *Am J*

586 *Bot.* 79: 1158 – 1161.

587

588 Marshall JD, Brooks JR, Lajtha K (2007) Sources of variation in the stable isotopic

589 composition of plants. In: Michener R and Lajtha K (eds)

590 *Stable isotopes in ecology and environmental science.*

591 Blackwell Publishing. Carlton, Victoria, pp 22 -60

592

593 Martínez-Cabrera HI, Estrada-Ruiz E (2014) Wood anatomy reveals high

594 theoretical hydraulic conductivity and low resistance to

595 vessel implosion in a cretaceous fossil forest from Northern

596 Mexico. *PloS One* 10:e108866-

597 doi:10.1371/journal.pone.0108866

598

599 Meinzer FC, Campanello PI, Domec J, Gatti MG, Goldstein G, Villalobos-Vega R,
600 Woodruff DR (2008) Constraints on physiological function
601 associated with branch architecture and wood density in
602 tropical forest trees. *Tree Physiol.* 28: 1609-1617.

603

604 O' Grady AP, Cook PG, Eamus D, Duguid A, Wischunsen JDH, Fass T, Worldege D
605 (2009) Convergence of tree water use within an arid-zone
606 woodland. *Oecologia.* 160: 643 – 655. doi: 10.1007/s00442-
607 009-1332-y

608

609 O'Grady AP, Eamus D, Cook PG, Lamontagne S (2006) Groundwater use by
610 riparian vegetation in the wet-dry tropics of northern
611 Australia. *Aust J Bot.* 54:145 – 154. doi:10.1071/BT04164

612

613

614 Pratt R, Jacobsen A, Ewers F, Davis S (2007) Relationships among xylem
615 transport, biomechanics and storage and roots of nine
616 Rhamnaceae species of the California chaparral. *New Phytol*
617 174: 787–798. doi: 10.1111/j.1469-8137.2007.02061.x

618

619 Pausas JG. Bark thickness and fire regime. *Funct Ecol* 29:315 –
620 327. doi:10.1111/1365-2435.12372

621

622 R Development Core Team (2008) R: A language and environment for statistical
623 computing. R Foundation for Statistical Computing, Vienna,
624 Australia. <http://www.R-project.org>.

625

626

627 Santini NS, Schmitz N, Bennion V, Lovelock CE (2012) The anatomical basis of
628 the link between density and mechanical strength in
629 mangrove branches. *Funct Plant Biol.* 40 : 400 – 408. doi:
630 <http://dx.doi.org/10.1071/FP12204>

631
632 Silvertown J (2004) Plant coexistence and the niche. *Trends Ecol Evol.* 19:605-
633 611. doi:10.1016/j.tree.2004.09.003
634
635 Silvertown J, Dodd ME, Gowing DJG, Mountford JO (1999) Hydrologically defined
636 niches reveal a basis for species richness in plant
637 communities. *Nature* 400:61-63. doi:10.1038/21877
638
639 Sterck F, Markesteijn L, Schieving F, Poorter L (2011) Functional traits
640 determine trade-offs and niches in a tropical forest
641 community. *PNAS* 108:20627 -20632.
642 doi:10.1073/pnas.1106950108
643
644 Tyree MT, Ewers FW (1991) The hydraulic architecture of trees and other
645 woody plants. *New Phytol.* 119:345-360. doi:10.1111/j.1469-
646 8137.1991.tb00035.x
647
648 Terradas J, Peñuelas J, Lloret F (2009) The fluctuation niche in plants.
649 *International Journal of Ecology* 2009: ID 959702, doi:
650 10.1155/2009/959702.
651
652 Scholz FG, Bucci SJ, Goldstein G, Meinzer FC, Franco AC, Miralles-Wilhelm (2007)
653 Biophysical properties and functional significance of stem
654 water storage tissues in Neotropical savanna trees. *Plant, Cell*
655 *Environ.* 30: 236 – 248. doi :10.1111/j.1365-
656 3040.2006.01623.x
657
658 Zanne A, Westoby M, Falster DS, Ackerly DD, Loarie SR, Arnold SEJ, Coomes DA
659 (2010) Angiosperm wood structure: Global patterns in vessel
660 anatomy and their relation to wood density and potential
661 conductivity. *Am J Bot.* 97: 207 – 215.
662 doi:10.3732/ajb.0900178
663

664 Zieminska K, Butler DW, Gleason SM, Wright IJ, Westoby M (2013) Fibre wall and
665 lumen fractions drive wood density variation across 24
666 Australian angiosperms AoB PLANTS 5: plt046;
667 doi:10.1093/aobpla/plt046
668
669
670
671
672
673
674
675
676
677
678
679
680
681
682
683
684
685
686
687
688
689
690
691
692
693
694
695
696
697
698
699
700
701
702
703
704
705

706
707
708
709
710
711
712

713 Tables

714 **Table 1.** Xylem characteristics, density of intact branches and wood density of different species of branches collected in the Ti Tree
715 Basin, Northern Territory. Values are means and standard errors, *n* indicates sample size. Different letters among columns indicate
716 means were significantly different $p < 0.05$ as tested with a one-way Analysis of Variance. A paired t-test was used to compare mean and
717 standard errors of density of intact branches and wood density within species.

718

719

Species	Paired t-test						
	Fibre wall thickness (μm)	Vessel wall thickness (μm)	Conductive area ($\text{mm}^2 \text{mm}^{-2}$)	Density of intact branches (g cm^{-3})	<i>n</i>	Wood density (g cm^{-3})	<i>n</i> p (t; df)
<i>E. vespertillo</i>	2.80 ± 0.11^A	1.98 ± 0.09^A	0.249 ± 0.020^{AB}	0.38 ± 0.03^A	9	0.40 ± 0.016	6 0.83 (0.22; 5)
<i>C. opaca</i>	3.36 ± 0.16^{AC}	2.88 ± 0.17^B	0.258 ± 0.032^{AB}	0.42 ± 0.08^{AB}	9	0.68 ± 0.022	6 0.02 (3.06; 5)
<i>E. camaldulensis</i>	3.31 ± 0.12^{AC}	2.61 ± 0.09^B	0.258 ± 0.053^B	0.51 ± 0.01^{BC}	9	0.65 ± 0.03	6 0.04 (2.6; 5)
<i>P. latifolia</i>	6.79 ± 0.42^B	3.78 ± 0.13^C	0.133 ± 0.013^{AC}	0.56 ± 0.02^{CD}	9	0.73 ± 0.017	6 0.0005 (7.9; 5)
<i>Hakea</i> sp.	4.26 ± 0.15^C	2.71 ± 0.13^B	0.123 ± 0.023^{AC}	0.65 ± 0.01^{DE}	9	0.719 ± 0.03	6 0.04 (2.7; 5)
<i>A. aneura</i>	4.01 ± 0.18^C	4.27 ± 0.19^C	0.098 ± 0.008^C	0.78 ± 0.01^{EF}	9	0.95 ± 0.07	6 0.03 (2.9; 5)
<i>A. bivenosa</i>	3.52 ± 0.20^{AC}	4.42 ± 0.17^C	0.099 ± 0.007^C	0.80 ± 0.03^E	9	0.88 ± 0.09	6 0.28 (1.2; 5)

720

721

722

723

724

725

726

727

728

729

730 **Table 2.** Values of $\delta^{13}\text{C}$ for leaves ($n = 9$ leaves per species) of six species collected in the Ti Tree Basin arid zone. Values are means and
731 standard errors. Different letters among columns indicate means were significantly different $p < 0.05$ as tested with a one-way Analysis
732 of Variance.

733

Species	$\delta^{13}\text{C}$ in leaves
<i>E. vespertillo</i>	-27.45 ± 0.07^A
<i>C. opaca</i>	-28.43 ± 0.47^{AB}
<i>E. camaldulensis</i>	-29.89 ± 0.41^B
<i>P. latifolia</i>	-26.50 ± 0.49^A
<i>Hakea</i> sp.	-26.84 ± 0.80^A
<i>A. aneura</i>	-26.96 ± 0.27^A

740

741

742

743

744

745

746

747

748

749 **Table 3.** Calculated means and standard errors of theoretical hydraulic conductivity (K_s), Vulnerability Index (VI) and vessel implosion
 750 resistance $(t/b)^2$, where t is the double-wall thickness (in μm) and b is the hydraulic mean vessel diameter (in μm). Different letters
 751 among columns indicate means were significantly different $p < 0.05$ as tested with a one-way Analysis of Variance.

Species	K_s ($\text{kg mm}^{-1} \text{MPa}^{-1} \text{s}^{-1}$)	VI	n	$(t/b)^2$	n		
<i>E. vespertillo</i>	0.383 ± 0.047	A	AC	9	0.0096 ± 0.00006	A	3
<i>C. opaca</i>	0.356 ± 0.058	A	A	9	0.0213 ± 0.00047	B	3
<i>E. camaldulensis</i>	0.328 ± 0.082	A	A	9	0.0237 ± 0.00001	B	3
<i>P. latifolia</i>	0.047 ± 0.006	B	B	9	0.14 ± 0.00092	C	3
<i>Hakea</i> sp.	0.08 ± 0.019	B	AB	9	0.0404 ± 0.00154	D	3
<i>A. aneura</i>	0.109 ± 0.017	B	C	9	0.059 ± 0.00009	E	3
<i>A. bivenosa</i>	0.099 ± 0.004	B	C	9	0.067 ± 0.00011	F	3

752

753

754

755

756

757

758

759

760

761

762

763

764 **Table S1.** Relative growth rate (RGR) of some of our studied species obtained from the literature. NA indicates that data were not
765 available in the literature.

766

Species	Relative Growth Rate (RGR, mg g ⁻¹ day ⁻¹)	Reference
<i>E. vespertillo</i>	41	Tomlinson et al. (2012)
<i>C. opaca</i>	N.A.	
<i>E. camaldulensis</i>	215	Grotkopp and Reimanek (2007)
<i>P. latifolia</i>	N.A.	
<i>Hakea</i> spp.	Range, 15 - 35	Poot and Lambers (2003)
<i>A. aneura</i>	59.5	Atkin et al. (1999)
<i>A. bivenosa</i>	N.A.	

767

768

769 **References**

770

771 Atkin OK, Schortemeyer M, McFarlane N, Evans JR (1999) The response of fast- and slow-growing Acacia species to elevated
772 atmospheric CO₂: an analysis of the underlying components of relative growth rate. *Oecologia*. 120 : 544 - 554.

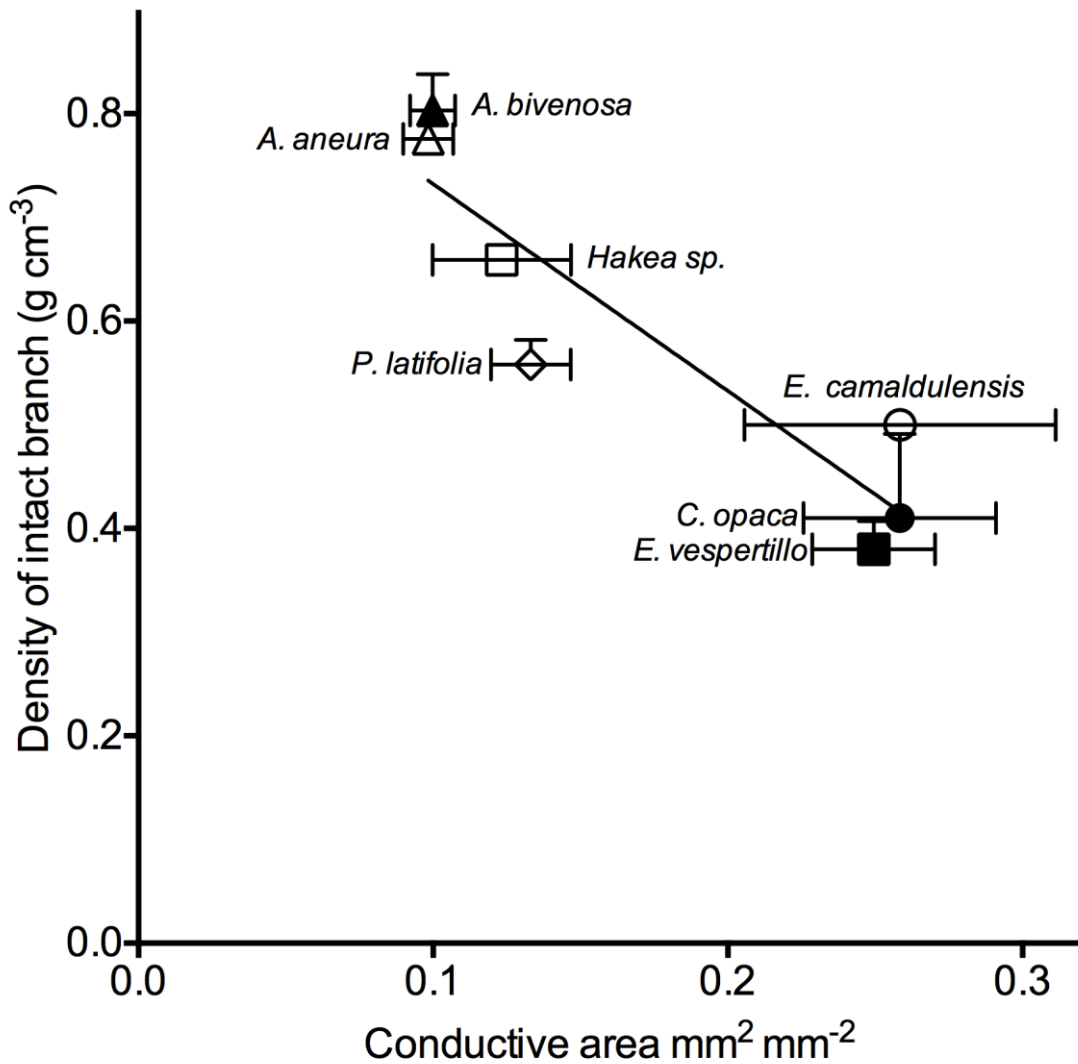
773

774 Tomlinson KW, Sterck FJ, Bongers F, da Silva DA, Barbosa ERM, Ward D, Bakker FT, van Kaauwen M, Prins HHT, de Bie S, van Langevelde
775 F (2012) Biomass partitioning and root morphology of savanna trees across a water gradient. *Journal of Ecology*.
776 100:1113 – 1121.

777

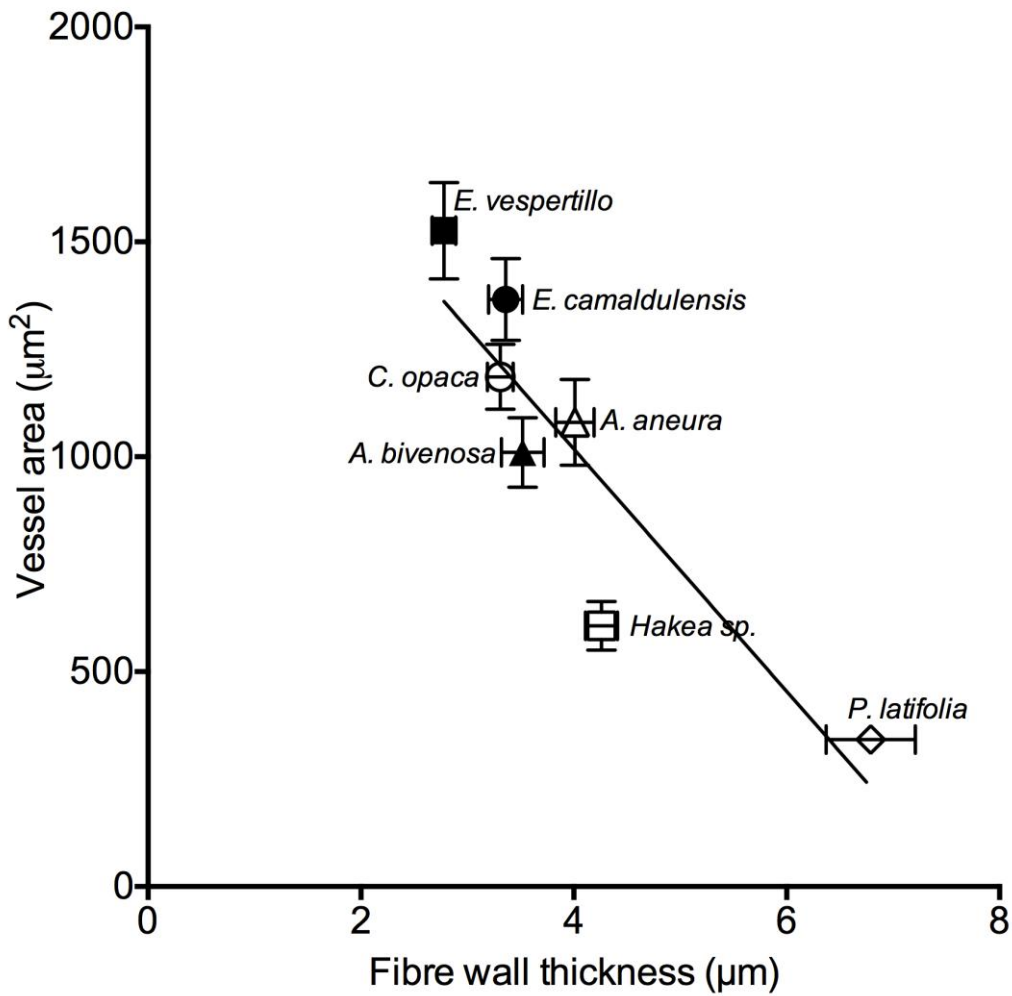
- 778 Grotkopp E, Rejmánek M (2007) High seedling relative growth rate and specific leaf area are traits of invasive species: Phylogenetically
779 independent contrasts of woody angiosperms. *American Journal of Botany*. 94: 526-532.
780
- 781 Poot P, Lambers H (2003) Growth responses to waterlogging and drainage of woody *Hakea* (Proteaceae) seedlings, originating from
782 contrasting habitats in south-western Australia. *Plant and Soil*. 253:57-70.

784 **Figure legends**
 785



786
 787 **Fig. 1.** Relationship between density of intact branch and conductive area
 788 ($r^2=0.83$; $p=0.004$) for seven co occurring species from the Ti Tree basin,
 789 Northern Territory. The regression was: Density of intact branch = -1.99
 790 Conductive area + 0.93.

791
 792
 793
 794
 795
 796
 797



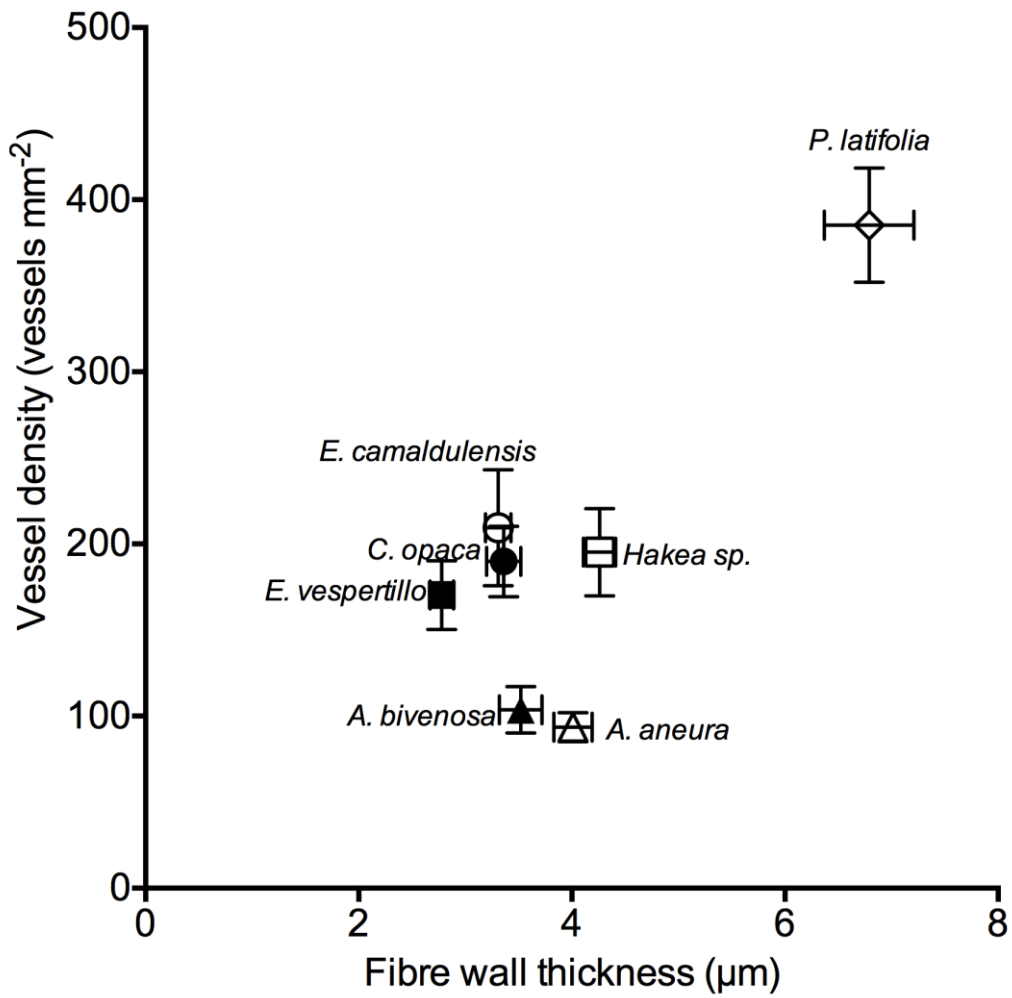
798

799

800 **Fig. 2.** Relationship between vessel area and fibre wall thickness ($r^2=0.80$;
 801 $p=0.006$) for seven co occurring species from the Ti Tree basin, Northern
 802 Territory. The regression was: Vessel area= -282 Fibre wall thickness + 2145.

803

804



805

806

807 **Fig. 3.** Relationship between vessel density and fibre wall thickness ($r^2=0.05$;

808 $p=0.67$) for six co occurring species from the Ti Tree basin, Northern Territory.

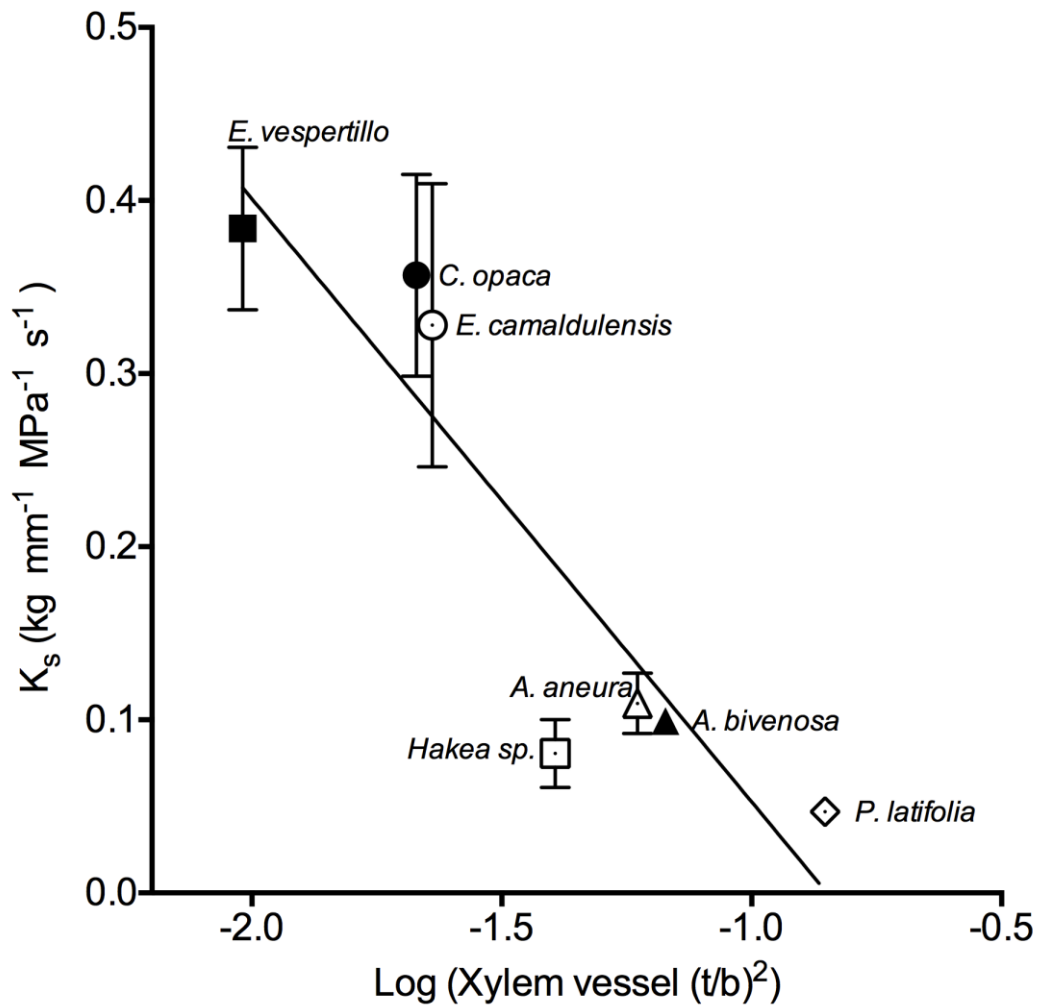
809

810

811

812

813



814

815

816 **Fig.4.** Relationship between theoretical hydraulic conductivity (K_s) and log
 817 xylem vessel implosion resistance $(t/b)^2$, the regression was $K_s = -0.3484$ xylem
 818 vessel $(t/b)^2 - 0.2958$ ($r^2=0.83$, $p=0.004$).

819

820

821

822

823

824

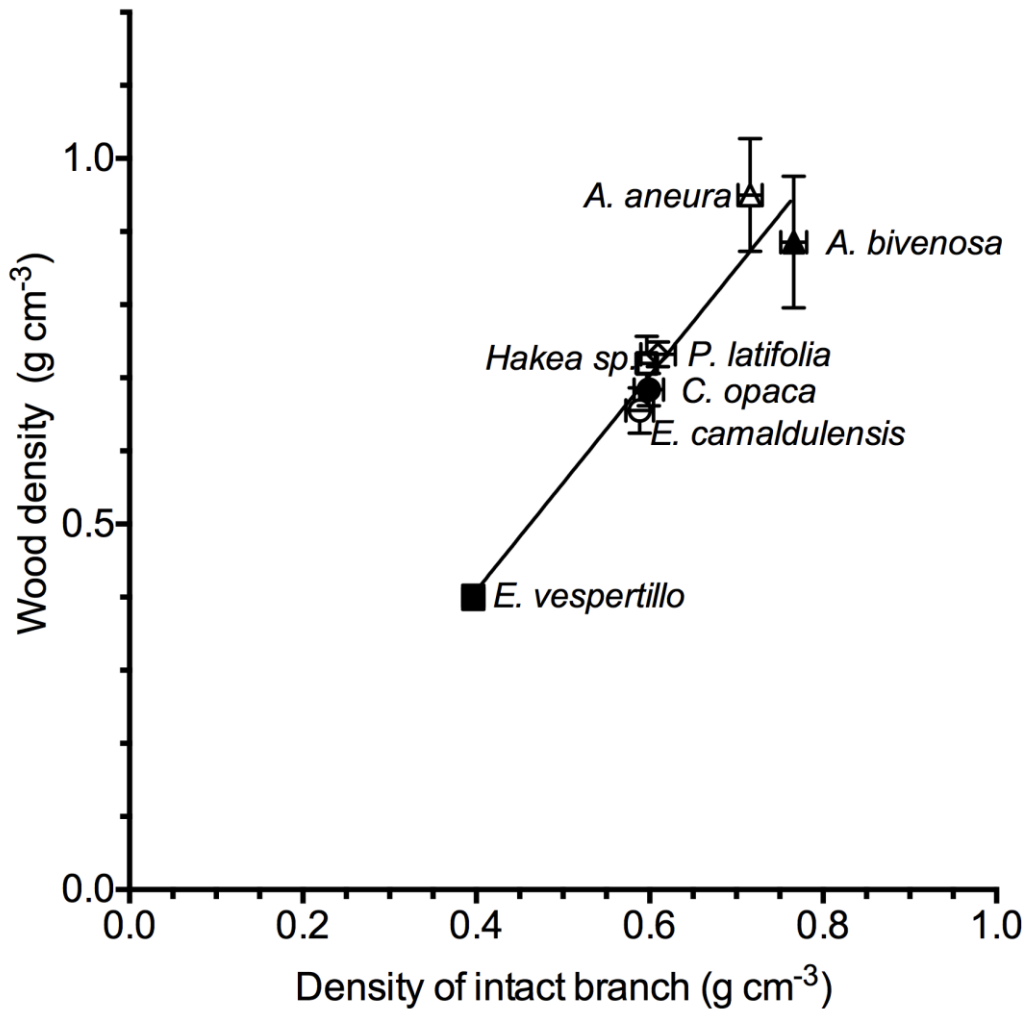
825

826

827

828

829

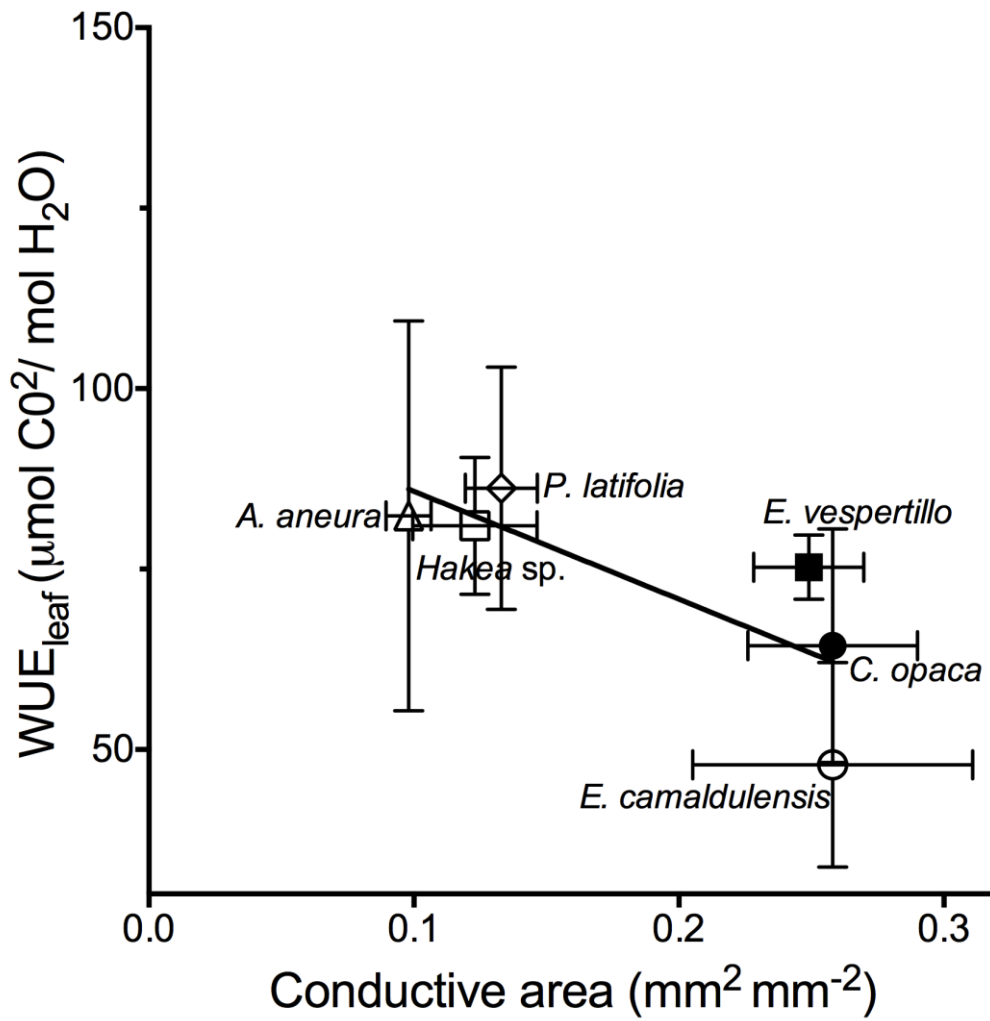


830

831 **Fig. 5.** Relationship between wood density and density of intact branch ($r^2=0.93$;
 832 $p=0.0003$) for seven co-occurring species from the Ti Tree basin, Northern
 833 Territory. The regression was: Wood density = 1.47 Density of intact branch -
 834 0.18.

835

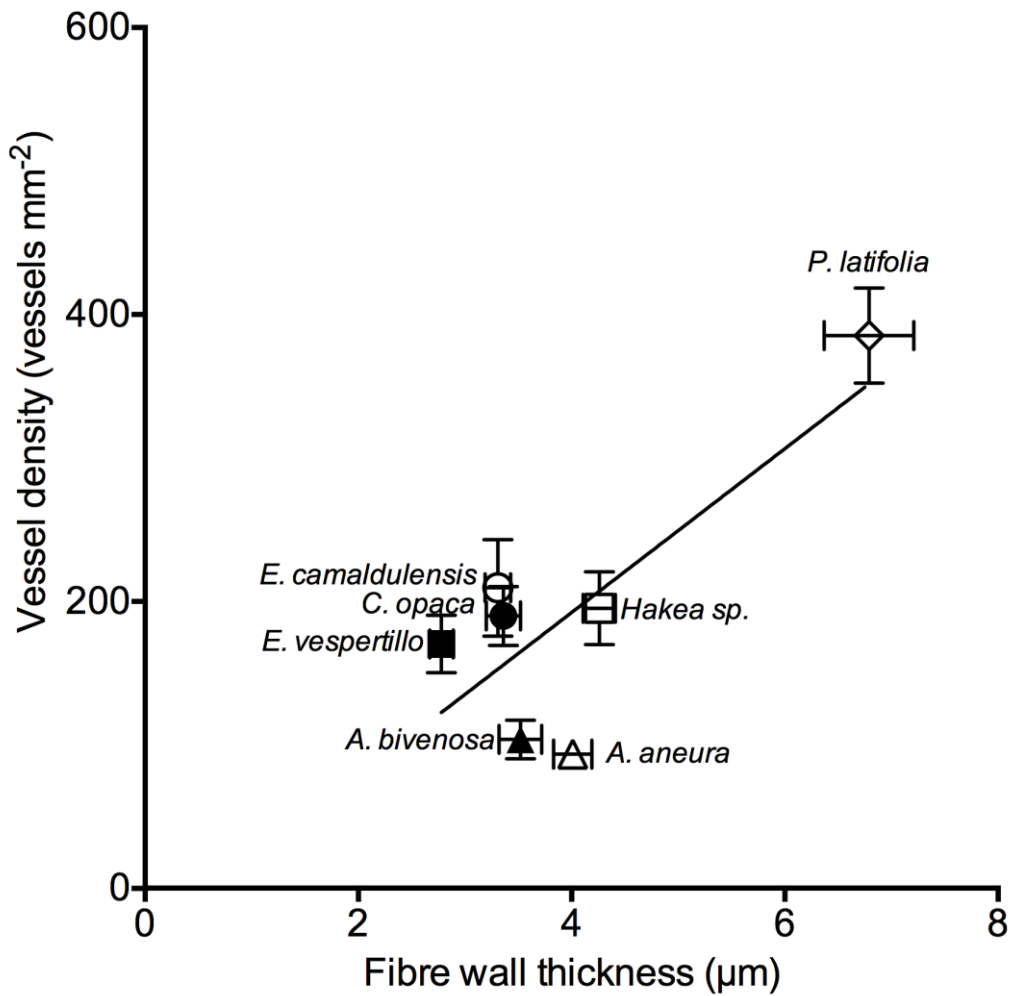
836



837

838 **Fig. 6.** Correlation between water use efficiency (WUE, obtained with $\delta^{13}\text{C}$ from
 839 leaves) and conductive area ($r^2=0.81$, $p<0.05$).

840



841

842 **Fig. S1.** Relationship between vessel density and fibre wall thickness ($r^2=0.61$;
 843 $p=0.037$) for seven co occurring species from the Ti Tree basin, Northern
 844 Territory. The regression was: Vessel density= 57.1 Fibre wall thickness - 36.23.

845

846

847

848

849

850

851

852

853

854

855

